

PROGRESS IN THE DESIGN OF THE FUTURE CIRCULAR COLLIDER FCC-ee INTERACTION REGION *

M. Boscolo^{†1}, G. Broggi^{1,2,4}, A. Ciarma¹, E. Di Pasquale¹, F. Franesini¹, S. Lauciani¹,
G. Nigrelli^{1,2}, F. Bosi³, F. Palla^{3,4}, K. D. J. André⁴, M. Benedikt⁴, R. Bruce⁴, H. Burkhardt^{4,9},
A. Frasca⁴, A. Lechner⁴, G. Lerner⁴, K. Oide⁴, F. Zimmermann⁴, A. Ilg⁵, M. Koratzinos⁶,
J. Seeman⁷, A. Novokhatski⁷, T. Raubenheimer⁷, P. Raimondi⁸

¹ INFN-LNF, Frascati, Italy ² Sapienza U., Rome, Italy ³ INFN-Pisa, Italy

⁴ CERN, Geneva, Switzerland ⁵ Uni. Zurich, Switzerland ⁶ PSI, Villigen, Switzerland

⁷ SLAC, Menlo Park, CA, USA ⁸ Fermilab, Batavia, IL, USA ⁹ Univ. Freiburg, Germany

Abstract

We report on the latest developments for the FCC-ee interaction region design that represents a major challenge for the collider, which has to achieve extremely high luminosity over a wide range of centre-of-mass energies. The FCC-ee will host four experimental apparatuses. We report on the progress of the mechanical model of the interaction region. The machine parameters have to be well controlled and the design of the machine-detector-interface has to be carefully optimized. In particular, the complex final focus hosted in the detector region has to be carefully designed, and the impact of beam losses and of any type of radiation generated in the interaction region, including beamstrahlung, have to be simulated in detail.

INTRODUCTION AND CONSTRAINTS

The MDI of the FCC-ee [1] is a compact and complex design that fulfils constraints given both by the machine and detector requirements. The FCC-ee optics varies with the beam energy to allow a common IR layout at all energies. The flexibility of the IR optics is obtained by splitting the first quadrupole into three segments and by modulating their sign and strength according to the beam energy. Tens of nanometers in the vertical beam size and few micrometer horizontally require small β -functions at the IP, down to 0.1 m and 0.8 mm at the Z pole respectively, that are obtained with a doublet of superconducting quadrupoles. The distance of the face of the final quadrupole from the IP is 2.2 m, residing inside the detector. The crab-waist collision scheme [2] requires a small vertical beam size and a large crossing angle at the IP, set to 30 mrad, which results with the beams entering/exiting with separate beam pipes at about 1.2 m from the IP. In addition to the optics constraints to the IR layout, the physics reconstruction benefits from a stay-clear cone of 100 mrad from the IP along the detector axis.

MDI LAYOUT

The MDI layout is shown in Fig. 1. Given the above constraints, the mechanical layout of the IR comprises a

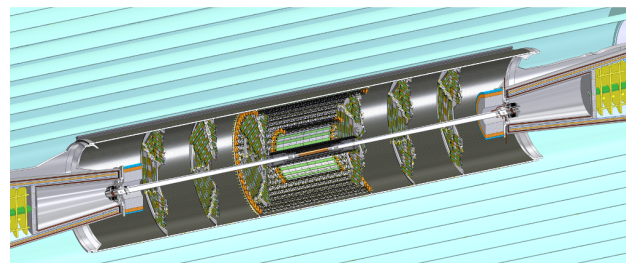


Figure 1: MDI overall layout. The support tube hosts the vertex and the luminosity detectors, the vacuum chambers and the bellows.

central beam pipe 18 cm long with a 10 mm internal radius and a pair of conical beam pipes about 1100 mm long on either side, as discussed in Ref. [3, 4]. The mechanical model of the IR vacuum chamber has to fulfill conflicting requirements: it must have a smooth shape to provide low impedance, it has to be as thin as possible to minimise the material budget as required by the physics performance and at the same time rigid enough to resist stresses, it has to be cooled to control the beam heat loads and possible losses and heat due to synchrotron radiation (SR).

The impedance was minimised by carefully designing the transverse section of the beam vacuum chamber, with a smooth transition from a circular to an elliptical transverse shape, as discussed in Ref. [5]. In addition, internally to the central chamber, a thin gold layer of 5 μm thickness is deposited to increase the electrical conductivity, thus reducing the effects of the wakefields. Recent studies on the heat load in the vacuum chamber have been refined adding new elements, such as bellows, BPM, and SR mask, in the IR vacuum chamber and simulation results are presented in Ref. [6]. The first estimate of heat load in the central vacuum chamber gives approximately 58 W, which is removed by flowing liquid paraffin in a thin 1 mm surrounding channel, resulting in an effective outer radius of 11.7 mm. The IR vacuum chambers material is AlBeMet162, an alloy of Be(62%):Al(38%), chosen for its high elastic modulus and low-density. The resulting material budget distribution for the vacuum chamber is shown in Fig. 2 as a function of the polar angle θ with respect to the beam line. The cooling manifolds of the conical chamber, previously made in cop-

* This work was partially supported by the EC HORIZON 2020 project FCC-IS, grant agreement No. 951754.

[†] manuela.boscolo@lnf.infn.it

per, have been redesigned in AlBeMet162 to mitigate the effects of low angle Bhabha scattered electrons, showering in the luminosity calorimeter (LumiCal) detector acceptance. The material budget is shown in Fig. 3.

The vertex detector is placed on top of the vacuum chamber: two thin Peek-based rings, anchored on either side at about 170 mm from the IP on the conical chamber, hold a conical carbon fibre structure supporting three layers of silicon vertex detectors located at about 13.7, 22.7, and 34.8 mm radii, as shown in Fig. 4.

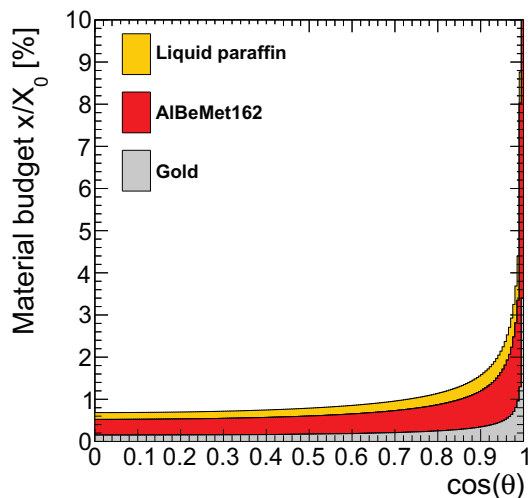


Figure 2: Material budget - in fraction of a radiation length (X_0) - of the central beam pipe as a function of the cosine of the polar angle with respect to the beam axis. The largest contribution is coming from the beam pipe walls in AlBeMet material.

Additional cylindrical layers and disks of silicon detectors complement the vertex detector in the reconstruction of charged particles.

The LumiCal, designed to measure the luminosity with an accuracy of 10^{-4} [7], sits just in front of the compensating solenoid at about 1074 mm and extends to 1190 mm from the IP. To achieve such a precision, the LumiCal has stringent mechanical requirements on its assembly and positioning, which result in constraining the MDI region. In particular the relative positioning of the two sides needs to be known with a precision of $\pm 110 \mu\text{m}$, implying that its mechanical stability down to that level must be ensured.

In addition, avoid spoiling the resolution, material must be minimised within its angular acceptance, comprised between 50 and 105 mrad with respect to the outgoing beam line.

All these elements are held in place by a lightweight carbon fibre and honeycomb rigid structure support tube which allows the overall integration before being inserted in the experiment.

The solenoidal magnetic fields of all the current detector concepts under study (IDEA, CLD, and ALLEGRO), have a strength of 2 T. Two 5 T compensation solenoids, placed between ± 1.23 and ± 2 m from the IP, cancel the magnetic

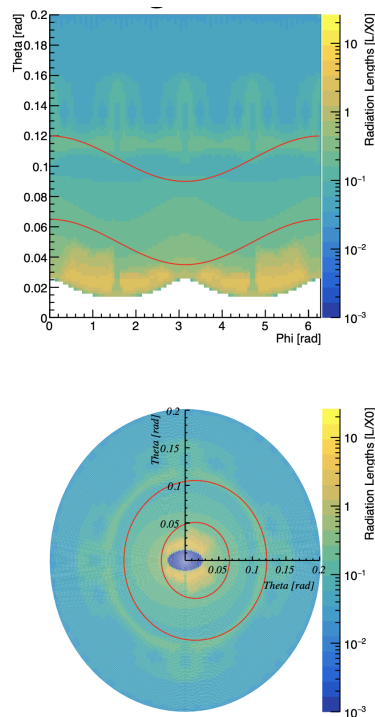


Figure 3: Material budget - in fraction of a radiation length (X_0 in log-scale) - of the central and conical beam pipes as a function of the azimuthal (Phi) and polar (Theta) angles (top) and in $x - y$ (bottom) in the detector reference system. The red lines indicate the envelop of the LumiCal, which is centered on top of the outgoing beam axis. The yellowish (high X_0) structures are the cooling manifolds: the largest contribution in the LumiCal acceptance is of nearly $0.5 X_0$ is at about 40 mrad polar angle, and the lowest at around 100 mrad.

field integral $\int B_z dz$ along the beam axis. Two 2 T solenoids are placed on either side around the final focus quadrupoles to screen the detector solenoidal field. This baseline scheme compensates the beam coupling resulting to an estimated vertical emittance growth of about 0.3 pm, to be compared to the nominal vertical emittance value of 1 pm.

An alternative solution for the coupling compensation is being proposed and described in Ref. [8], resulting in a vertical emittance growth of only 0.02 pm. It consists in moving the compensating solenoids that cancel the longitudinal field integral at approximately ± 20 m from the IP. A skew quadrupolar component is added to the final focus quadrupoles, aligning the magnet axis to the rotated reference frame of the beam. The orbit distortion generated by the horizontal crossing angle in the detector field is compensated by correctors placed right after the beam pipe separation and around the final focus quadrupoles.

The IR magnet system includes the final doublet, the coupling compensation solenoids, the correctors for IP fine tuning. Some of the following design aspects related to such a system are being addressed: the magnetic coil configurations, the mechanical support and electromagnetic force

management, cryogenic cooling, thermal shielding and associated heat loads of the warm beam pipe, quench detection, the interface with the IR BPM, the alignments system. A critical issue for the IR magnet system design is the space budget, especially inside the main superconducting quadrupole coils.

The final focus IR quadrupole magnet designs are presently based on the canted cosine theta (CCT) coil. A prototype conductor-in-grooves of one segment of the first final focus quadrupole was fabricated, and recently cold tests have been successfully performed and are presented in [9].

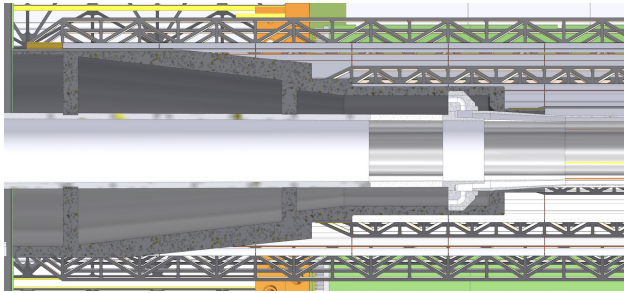


Figure 4: Longitudinal section of the beam pipe and the inner vertex. The dark gray object is the conical support of the vertex detector, which is supported by the conical beam pipe. At the right edge of the support cone, the inlet/outlet paraffine cooling manifolds are visible.

BEAM INDUCED BACKGROUNDS

The beam induced background sources can be described by two main categories: those single beam induced and those generated at the IP. Currently, among the former, we have studied SR [10] with BDSIM [11] utilising the GEANT4 [12] toolkit, halo beam losses [13] with Xsuite [14], while for the latter the Incoherent Pairs Creation (IPC) [15] with GuineaPig [16] and radiative bhabhas [17]. Ongoing efforts are in progress to implement the beam-gas scattering in X-Suite, followed by Touschek and thermal photons.

A model of the MDI area is being implemented in Fluka to establish fluences and Total Ionization Doses (TID) important for the electronics sitting inside and in the vicinity of the experimental halls. First estimates have been obtained of the power deposited in key machine elements, such as the Beamstrahlung dump, as well as the cumulative radiation levels in the tunnel [18]. These studies will be followed by the computation of the power deposited on the first final focus quadrupole and of the TID and fluences in the active detector elements.

The main sources of background from SR come from the last dipole magnet before the IP, the solenoid fringe field, and the final focus quadrupoles, considering also the non-Gaussian beam tails. The SR produced by the last dipole is efficiently stopped by carefully positioned collimators, that effectively protect the central chamber and masks from excessive synchrotron radiation flux, thereby reducing heat load and scattering near the IP. Two tungsten SR masks are

foreseen at the exit of the two final focus quads, QC2, and QC1, in order to intercept the SR emitted in the quads. This scheme guarantees a negligible amount of photons in the detector.

A first investigation of the effect of the energy deposition in the final focus quadrupoles, next to the IP, due to the radiative Bhabha background has been performed with FLUKA simulations using a simplified geometry model. The expected power densities are of the order of a few tens of mW/cm^3 and peak annual cumulative doses of the order of tens of MGy/y in the magnet coils for Z-pole operation (and lower levels for the other collision energies). Despite being preliminary and design-dependent, these estimates indicate that there is a concrete risk of magnet quenches and lifetime degradation (particularly at the Z-pole) requiring the implementation of dedicated solutions.

The IPC contribution influences mostly the vertex detectors which are located close to the beam pipe. The $e^+ - e^-$ pairs generate hits in the vertex detectors at a maximum level of about $400 \text{ MHz}/\text{cm}^2$ in the innermost vertex detector layer at the Z collision energy, challenging the electronic readout.

Studies are ongoing to estimate the background effect on other detector elements such as the drift chambers and electromagnetic calorimeters of IDEA and ALLEGRO detector concepts.

MDI MOCK-UP

A full scale mock up of the interaction region is in preparation at INFN Frascati, to prove the validity of the mechanical designs and allow the study of integration and services in this crowded area. A first goal will be to gather experience on the paraffine cooling system, which needs to be integrated together with the silicon vertex detector air-cooling manifolds. The mock-up will also serve to validate any interference between the LumiCal and the bellows, as well as the assembly sequence. Finally, a buckling test of the vacuum chambers will be performed.

CONCLUSIONS

The FCC-ee IR design requires challenging solutions to accommodate accelerator and detector elements in a very compact region. Intense and energetic beams impose special care to handle heat load, obtained by proper low-impedance and cooled IR vacuum chambers, special IR bellows with high-order-modes absorbers, and SR masks.

The high luminosity produces a high rate of IPC backgrounds, posing challenges to the sub-detector electronics. A new mechanical model of the vacuum chambers has been implemented to reduce the beam induced backgrounds in the LumiCal. Progress in the integration of the vertex and the beam pipe has been made, accommodating difficult routing of the cables and cooling piping. A full-scale mockup is being prepared to validate the design.

REFERENCES

- [1] A. Abada *et al.* [FCC], “FCC-ee: The Lepton Collider: Future Circular Collider Conceptual Design Report Volume 2”, *Eur. Phys. J. ST*, vol. 228, no.2, pp. 261-623, 2019. doi:10.1140/epjst/e2019-900045-4
- [2] M. Zobov, D. Alesini, M. E. Biagini, C. Biscari, A. Bocci, M. Boscolo, F. Bossi, B. Buonomo, A. Clozza and G. O. Delle Monache, *et al.* “Test of crab-waist collisions at DAFNE Phi factory”, *Phys. Rev. Lett.*, vol. 104, p. 174801, 2010. doi:10.1103/PhysRevLett.104.174801
- [3] M. Boscolo, H. Burkhardt, K. Oide, and M. K. Sullivan “IR challenges and the machine detector interface at FCC-ee”, *Eur. Phys. J. Plus*, vol. 136, no. 10, p. 1068, 2021. doi:10.1140/epjp/s13360-021-02031-5
- [4] F. Franesini *et al.*, “Mechanical design, structural requirements and optimization of the FCC-ee interaction region components”, presented at IPAC’24, Nashville, TN, USA, May 2024, this conference.
- [5] A. Novokhatski, M. Boscolo, F. Franesini, S. Lauciani, and L. Pellegrino, “Estimated heat load and proposed cooling system in the FCC-ee Interaction region beam pipe”, in *Proc. IPAC’23*, Venice, Italy, May 2023, pp. 260–263. doi:10.18429/JACoW-IPAC2023-MOPA092
- [6] A. Novokhatski *et al.*, “The design and electromagnetic analyses of the new elements in the FCC-ee IR beam vacuum chamber”, presented at IPAC’24, Nashville, TN, USA, May 2024, this conference.
- [7] M. Dam, “Challenges for FCC-ee luminosity monitor design,” *Eur. Phys. J. Plus*, vol. 137, no. 1, p. 81, 2022. doi:10.1140/epjp/s13360-021-02265-3
- [8] A. Ciarma *et al.*, “Alternative Solenoid Compensation Scheme for the FCC-ee Interaction”, presented at IPAC’24, Nashville, TN, USA, May 2024, this conference.
- [9] A. Thabuis and M. Koratzinos, “The first FCC-ee final focus quadrupole prototype”, presented at IPAC’24, Nashville, TN, USA, May 2024, this conference.
- [10] K.D.J. André, B. Holzer, and M. Boscolo, “Status of the Synchrotron Radiation studies in the Interaction region of the FCC-ee”, presented at IPAC’24, Nashville, TN, USA, May 2024, this conference.
- [11] L.J. Nevay *et al.*, “BDSIM: An Accelerator Tracking Code with Particle-Matter Interactions,” *Computer Physics Communications*, vol. 252, p. 107200, 2020.
- [12] J. Allison *et al.* “Recent developments in Geant4”, *Nucl. Instrum. Meth. A*, vol. 835, pp. 186-225, 2016. doi:10.1016/j.nima.2016.06.125
- [13] G. Broggi *et al.*, “Optimizations and updates of the FCC-ee collimation system design”, presented at IPAC’24, Nashville, TN, USA, May 2024, this conference.
- [14] A. Abramov *et al.*, “Collimation simulations for the FCC-ee”, *JINST*, vol. 19, p. T02004, 2024. doi:10.1088/1748-0221/19/02/T02004
- [15] A. Ciarma, M. Boscolo, G. Ganis, and E. Perez, “Machine Induced Backgrounds in the FCC-ee MDI Region and Beamstrahlung Radiation”, in *Proc. 65th ICFA Adv. Beam Dyn. Workshop High Luminosity Circular e+e- Colliders (eeFACT’22)*, Frascati, Italy, Sep. 2022, pp. 85–90. doi:10.18429/JACoW-eeFACT2022-TUZAT0203
- [16] D. Schulte, “Study of Electromagnetic and Hadronic Background in the Interaction Region of the TESLA Collider”, Ph.D. thesis, University of Hamburg, Rep. TESLA-97-08, 1996.
- [17] R. Kleiss and H. Burkhardt, “BBBREM: Monte Carlo simulation of radiative Bhabha scattering in the very forward direction”, *Comput. Phys. Commun.*, vol. 81, p. 372, 1994. doi:10.1016/0010-4655(94)90085-X
- [18] A. Frasca *et al.*, “Energy deposition and radiation level studies for the FCC-ee experimental insertions”, presented at IPAC’24, Nashville, TN, USA, May 2024, this conference.